

MG53 attenuates nitrogen mustard-induced acute lung injury

Haichang Li¹  | Lucia Rosas² | Zhongguang Li¹ | Zehua Bian¹ | Xiuchun Li¹ |
Kyoungan Choi¹ | Chuanxi Cai¹ | Xinyu Zhou¹ | Tao Tan¹ | Valerie Bergdall³ |
Bryan Whitson¹ | Ian Davis² | Jianjie Ma¹

¹Department of Surgery, The Ohio State University, Columbus, Ohio, USA

²Department of Veterinary Biosciences, The Ohio State University, Columbus, Ohio, USA

³Department of Veterinary Preventive Medicine, The Ohio State University, Columbus, Ohio, USA

Correspondence

Jianjie Ma, Department of Surgery, The Ohio State University, Columbus, OH, USA.

Email: Jianjie.ma@osumc.edu

Funding information

Ohio State University; National Institutes of Health, Grant/Award Number: R01AG056919, R01AR070752, R01DK106394, R01HL137090 and R01HL143000; Department of Defense, Grant/Award Number: W81XWH1810787

Abstract

Nitrogen mustard (NM) is an alkylating vesicant that causes severe pulmonary injury. Currently, there are no effective means to counteract vesicant-induced lung injury. MG53 is a vital component of cell membrane repair and lung protection. Here, we show that mice with ablation of MG53 are more susceptible to NM-induced lung injury than the wild-type mice. Treatment of wild-type mice with exogenous recombinant human MG53 (rhMG53) protein ameliorates NM-induced lung injury by restoring arterial blood oxygen level, by improving dynamic lung compliance and by reducing airway resistance. Exposure of lung epithelial and endothelial cells to NM leads to intracellular oxidative stress that compromises the intrinsic cell membrane repair function of MG53. Exogenous rhMG53 protein applied to the culture medium protects lung epithelial and endothelial cells from NM-induced membrane injury and oxidative stress, and enhances survival of the cells. Additionally, we show that loss of MG53 leads to increased vulnerability of macrophages to vesicant-induced cell death. Overall, these findings support the therapeutic potential of rhMG53 to counteract vesicant-induced lung injury.

KEYWORDS

acute lung injury, MG53, nitrogen mustard, oxidative stress

1 | INTRODUCTION

Sulphur mustard (SM) and nitrogen mustard (NM) are alkylating agents known to cause severe damage to organs including the skin, eyes, lungs and nervous system, among which pulmonary toxicity is the major cause of death.¹ Pulmonary toxicity involves complicated cellular events, including DNA damage, oxidative stress, acute injury and inflammation.²⁻⁴ In those who survive vesicant exposure, progressive inflammation often leads to pulmonary fibrosis and prolonged respiratory dysfunction.⁵⁻⁸

Pulmonary exposure to SM/NM induces alkylating injuries with an acute and a chronic injury phase. The acute lung injury develops due

to oxidative stress, lipid peroxidation and liberation of inflammatory mediators.⁹⁻¹¹ The prolonged injury is mediated by chronic inflammation and fibrotic remodelling in the upper and small airways.^{12,13} Despite many studies investigating the mechanism of mustard-induced lung injury, current therapies to treat mustard poisoning are mostly palliative.^{4-8,14-19} Therapeutic means that mitigate acute oxidative stress, harness inflammation and restore cell membrane integrity could potentially alleviate the deleterious impact of vesicant and other environmental insults in the lung.

MG53 is a member of the TRIM protein (TRIM72), which functions as an essential component of plasma membrane repair.^{20,21} MG53 knockout mice (*mg53*^{-/-}) develop pulmonary pathology due

Haichang Li, Lucia Rosas equal contributors.

This is an open access article under the terms of the Creative Commons Attribution License, which permits use, distribution and reproduction in any medium, provided the original work is properly cited.

© 2022 The Authors. *Journal of Cellular and Molecular Medicine* published by Foundation for Cellular and Molecular Medicine and John Wiley & Sons Ltd.

to defective membrane repair.²² We have shown that the recombinant human MG53 protein (rhMG53) when administered either intravenously (IV) or via aerosol has the ability to effectively mitigate lung ischaemia-reperfusion injury, lipopolysaccharide-induced inflammation and porcine pancreatic elastase (PPE)-induced emphysema in rodents and pigs.²³ In addition to membrane repair, recent studies demonstrate an anti-inflammatory function of MG53 in dampening NF- κ B signalling, and knockdown of MG53 leads to hyper-inflammation in human macrophages.^{24,25}

Herein, we provide data to support the physiologic function of MG53 in lung protection and the potential therapeutic value of rhMG53 to treat vesicant-induced lung injury. When compared to wild-type littermates, *mg53*^{-/-} mice display an exacerbated lung injury with a more severe lung dysfunction following exposure to NM. Additionally, we show that intravenous administration of rhMG53 to wild-type mice after exposure to NM can mitigate the adverse effects of NM-vesicant lung injury.

2 | MATERIALS AND METHODS

2.1 | Regents and recombinant human MG53 protein (rhMG53)

NM (Mechlorethamine hydrochloride) was purchased from Sigma-Aldrich Chemicals Co. (St. Louis, MO). rhMG53 protein was purified from *E. coli* fermentation as described previously.²⁶

2.2 | Animals and animal treatment

All animal care and usage were done in accordance with federal policies and guidelines and approved by the Ohio State University's IACUC. *mg53*^{-/-} mice, tPA-MG53 and their *wild-type* littermates were bred and generated as previously described.^{20,27} Mice were anaesthetized by intraperitoneal (IP) injection of ketamine and xylazine (80 mg/kg; 10 mg/kg, respectively) and then were treated with PBS or NM (0.125 mg/kg) by intratracheal instillation following the protocol as described previously with minor modification.² NM was prepared immediately before administration. All procedures were performed in a designated room with chemical hood strictly following OSU Environment and Health and Safety guidelines. rhMG53 (2 mg/kg) in saline or saline alone was administered by daily IV injection right after NM treatment for five days.

2.3 | Cells, cell culture and stress treatment

Human bronchial epithelial cells (B2B) and THP-1 cells were purchased from the American Type Culture Collection (ATCC). The B2B and THP-1 cells were grown in RPMI 1640 medium supplemented with 10% FBS, 100 U/ml penicillin and 100 μ g/ml streptomycin at 37°C in the presence of 5% CO₂. The sh-MG53-knockdown THP-1

cells were created and cultured as described previously.²⁴ Primary porcine aortic endothelial cells (PAoEC) were isolated as previously described²⁸ and cultured in MEM containing 10% FBS, 2 mM glutamine, 100 U/ml penicillin and 100 μ g/ml streptomycin (Lonza) with bovine brain extract at 37°C in the presence of 5% CO₂.

2.4 | Apoptosis assay and ROS measurement

Cell apoptosis was investigated by dual staining with Alexa Fluor 488 annexin V and propidium iodide (PI) (Invitrogen Cat# V13241) following the manufacture protocol. Briefly, PAoEC and B2B cells were seeded in 6-well plates, cultured for 24 h and then incubated with 10 μ M (for PAoEC)/20 μ M (for B2B cells) NM or BSA control for 4 h, washed and incubated with BSA or rhMG53 (10 μ g/ml) for another 20 h. Cells were detached by 0.25% trypsin-EDTA solution and washed with PBS for 1 time, and Annexin V and PI staining were performed for FACS analysis and analysed as described previously.²⁹

Cellular-reactive oxygen species (ROS) production was measured using a ROS Detection Assay Kit (Abcam Cat#ab113851) according to manufacture instructions. Briefly, cells were seeded in 6-well plates, cultured for 24 h and then incubated with 10 μ M (for PAoEC)/20 μ M (for B2B cells) NM or BSA control for 4 h, and washed with PBS, incubated with BSA or rhMG53 (10 μ g/ml) and cultured for another 20 h. Cells were washed, stained and analysed with DCF staining. The intensity of red fluorescence was detected by Guava EasyCyte™ System, and images were taken by confocal microscope.

2.5 | Lung function measurement

Mice were anaesthetized by intraperitoneal (IP) injection of diazepam (17.5 mg/kg) followed by ketamine (80 mg/kg), and lung mechanics were assessed as previous described.³⁰ Briefly, mouse was mechanically ventilated on a computer-controlled flexiVent FX piston ventilator (SciReq; Montreal, Canada), with a tidal volume of 10 ml/kg at a frequency of 200 breaths/minute, against 2–3 cmH₂O PEEP, as in our previous studies. Following two total lung capacity manoeuvres to standardize volume history, basal airway resistance and dynamic lung compliance were measured by the forced oscillation technique.³¹

2.6 | Antibodies and western blotting

Primary antibodies used in this study are as follows: anti-cleaved caspase-3 (Cell Signaling Technologies) and anti-GAPDH (Santa Cruz Biotechnology). Total protein extractions were prepared and subjected to immunoblot analysis as described previously.^{32,33} Briefly, after blocking, membranes were incubated with relevant antibodies and probed with corresponding HRP-conjugated secondary antibodies (Cell Signaling Technologies). All films were developed with ECL-Plus reagents (GE healthcare) and imaged using ChemiDoc™ Gel Imaging System (Bio-Rad).

2.7 | Cell membrane injury assay and confocal microscopy

For membrane repair assay, B2B cells were transfected with GFP-MG53 and then subjected to microelectrode penetration-induced acute cell membrane injury, and the data were analysed as previously described.²⁰

2.8 | Histology and immunofluorescent staining

Histology and immunofluorescent staining were performed as previously described.^{32,33} Briefly, tissues were dissected from experimental animals and then fixed in 4% paraformaldehyde (PFA) overnight at 4°C. After fixing, samples were washed three times for 5 min with 70% ethanol. Washed samples were processed, embedded in paraffin. 4 µm thick paraffin sections were cut. Cells were fixed with 4% PFA.

2.9 | Statistical analysis

All data are expressed as means ± standard error of mean (SEM). Statistical evaluation was conducted using the student's *t* test and by ANOVA for repeated measures. A value of *p* < 0.05 was considered statistically significant.

3 | RESULTS

3.1 | Mg53^{-/-} mice are more susceptible to NM-induced lung injury

To understand the physiological role of MG53 in protection against vesicant-induced lung injury, we administered NM (0.125 mg/kg) intratracheally (IT) to *mg53*^{-/-} mice and *wild-type* littermate controls, according to the protocol developed by Laskin and colleagues.² At 5 days post-NM exposure, more severe lung damage was observed in *mg53*^{-/-} mice than in *wild-type* mice (Figure 1A). While carotid arterial oxygen saturations (SaO₂) only showed a marginal difference between *wild-type* and *mg53*^{-/-} mice (Figure 1B), significant elevations of airway resistance (R_{rs}, Figure 1C) and compromised lung dynamic compliance (C_{dyn}, Figure 1D) were observed in the *mg53*^{-/-} mice. Histological analysis revealed massive parenchymal necrosis with increased infiltration of immune cells in the *mg53*^{-/-} lung (Figure 1E).

These observations are consistent with our recent findings that *mg53*^{-/-} mice experience worsened morbidity and delayed recovery compared to *wild-type* mice in a non-lethal infection with influenza virus, correlating with increased inflammatory pathology in the lungs of the *mg53*^{-/-} mice.²⁴ Together, these data demonstrate that genetic ablation of MG53 renders the mice more susceptible to vesicant-induced lung dysfunction and inflammation.

3.2 | rhMG53 mitigates NM-induced lung injury in mice

We recently reported that recombinant human MG53 protein (rhMG53) protects mice from lethal influenza virus infection and could function as a therapeutic to treat inflammation-driven infectious diseases.²⁵ To determine whether rhMG53 has similar protective effects against chemical lung injury, C57BL/6J mice (10 weeks age) were exposed to NM (0.125 mg/kg, IT) to induce lung injury. Mice were divided into two groups, one receiving tail vein administration of 2 mg/kg rhMG53 protein right after NM exposure (and then daily thereafter), and the others receiving saline as control at the same frequency with analysis conducted in a blinded manner. Mice receiving saline showed progressive decline of body weight, which was mitigated by rhMG53 treatment during the 5-day observation period (Figure 2A, left). Out of the 4 mice in the control group, one died on day 2, while all rhMG53-treated mice survived the 5 days observation period.

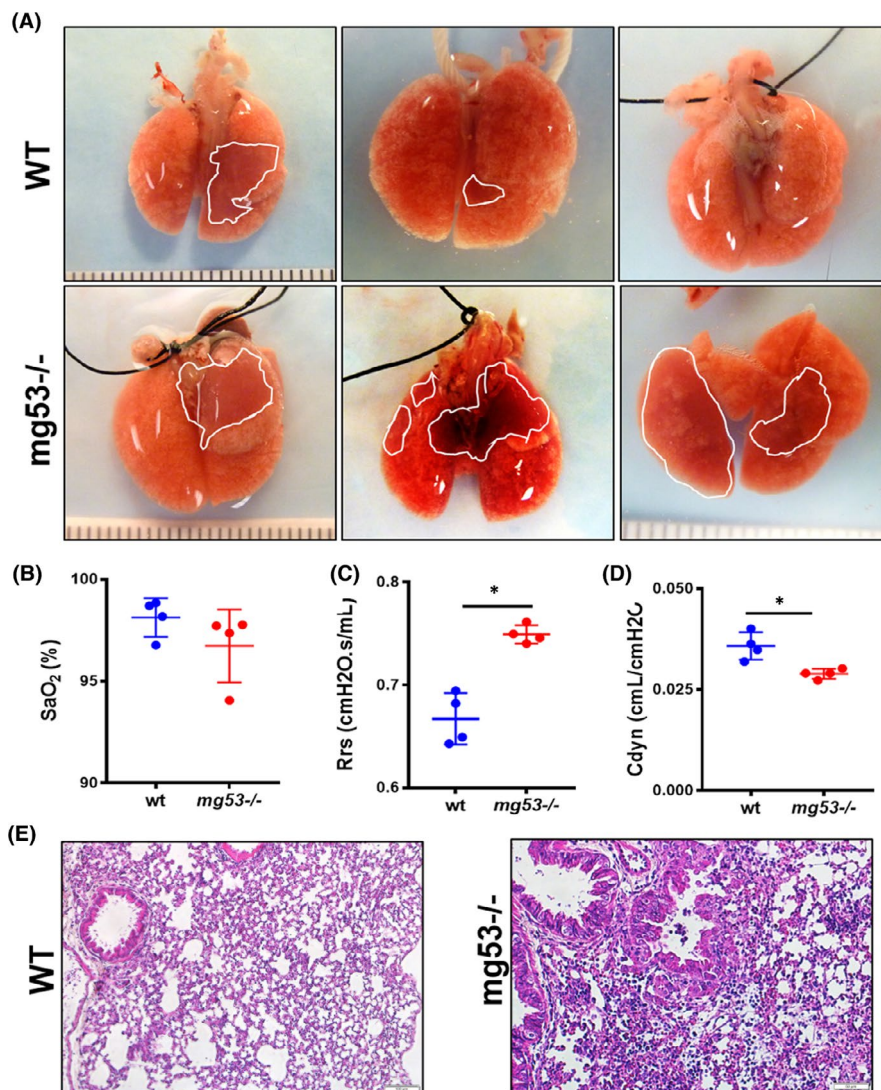
We have generated a transgenic mouse model with sustained elevation of MG53 level in the bloodstream (tPA-MG53). Transgenic mice with baseline overexpression and secretion of increased levels of MG53 in the bloodstream (tPA-MG53) live a healthier and longer life than littermate *wild-type* mice. Western blot confirmed ~100-fold elevation of MG53 in serum from the tPA-MG53 mice compared with *wild-type* littermates. tPA-MG53 mice display remarkable wound-healing capacity and improved injury repair and regeneration.³⁴ Compared with the *wild-type* mice, the tPA-MG53 mice experienced less weight loss after NM treatment (Figure 2A, right).

At the gross level, lung injury appeared less severe in rhMG53-treated mice compared with the control group 5 days after NM exposure (Figure 2B). Even with the limited number of animals, we observed that rhMG53 treatment led to improved oxygen saturation (SaO₂, Figure 2C) and trended towards increased dynamic lung compliance (C_{dyn}, Figure 2D) and reduced airway resistance (R_{rs}, Figure 2E).

3.3 | NM exposure impairs MG53-mediated membrane repair in lung epithelial cells

To understand the mechanism that underlies MG53's role in protection against NM-induced lung injury, we conducted in vitro membrane repair assay as described previously.^{20,22} Human lung epithelial (B2B) cells were transfected with GFP-MG53 and treated with BSA vehicle or 10 µM NM. At 24 h after transfection, confocal fluorescence live-cell imaging was conducted. As shown in Figure 3A, there were remarkable changes in the subcellular distribution of GFP-MG53 in B2B cells treated with NM. GFP-MG53 shows a plasma membrane localization pattern in control conditions, which was expected for the membrane repair-patch function of MG53 (as observed in many other cell types^{20,26,32}). However, GFP-MG53 was

FIGURE 1 Knockout of MG53 enhances NM-induced lung injury. Mice were treated by intratracheal instillation of either 50 μ l NM (0.125 mg/kg in saline) or 50 μ l saline alone. After 5 days of exposure, the lung function was examined, and mice were euthanized for lung tissue section preparation. (A) Representative images of *wild-type* (upper panels) and *mg53^{-/-}* (lower panels) lung subjected NM exposure. Quantification of the lung function with blood oxygen saturation level (SaO₂) (B), and resistance (Rrs) (C) and dynamic compliance (C_{dyn}) (D). (E) Histological analyses revealed massive necrosis with increased infiltration of immune cells in the *mg53^{-/-}* lung (right panel). These data demonstrate that ablation of MG53 renders the mice more susceptible to NM-induced lung injury. * $p < 0.05$ for the indicated group



mostly present in soluble and aggregated forms in the cytoplasm of B2B cells treated with NM.

Microelectrode poking induces acute injury to the plasma membrane of B2B cells, resulting in rapid translocation and accumulation of GFP-MG53 at the site of injury for repair-patch formation. The repair patch remained stable over the 2 min observation period in control cells not exposed to NM (Figure 3B, green). Remarkably, B2B cells treated with NM displayed dysfunctional GFP-MG53 movement following microelectrode induced membrane injury (Figure 3B, red). While there was an initial small accumulation of GFP-MG53 at the injury site within the first 30 s after injury, the repair patch did not remain stable as this decreased within the 2 min recording period.

Using FM1-43 dye entry as a direct measure of cell membrane integrity,^{20,26} we found that exposure of B2B cells to NM caused more entry of FM1-43 dye, which could be reduced by treatment with rhMG53 (5 μ g/ml) (Figure 3C,D). These findings provide direct evidence that vesicant exposure of lung epithelial cells leads to disruption of cell membrane repair machinery.

3.4 | rhMG53 protects lung epithelial as well as endothelial cells against NM-induced injury

Studies show that SM/NM exposure leads to elevation of cellular oxidative stress.^{6,10,11,35,36} We have demonstrated before that MG53's membrane repair function is impaired when cells are subjected to chronic oxidative stress.^{37,38} We next conducted a series of studies to quantify the potential protective role of rhMG53 in mitigating NM-induced oxidative stress and injury to B2B cells. We used DCF fluorescent indicator to quantify intracellular ROS level and observed a significant increase in DCF fluorescence in B2B cells treated with 50 μ M NM for 2 h (Figure 4A). FACS analysis was used to quantify the changes in ROS levels in B2B cells treated with NM (+saline) and NM (+rhMG53) (Figure 4B). rhMG53 treatment (5 μ g/ml) significantly suppressed the NM-induced elevation of ROS in B2B cells (Figure 4C).

Our laboratory has developed a protocol to isolate primary porcine aortic endothelial cells (PAoEC), which are widely used as an in vitro system to evaluate endothelial cell function (of either aortic

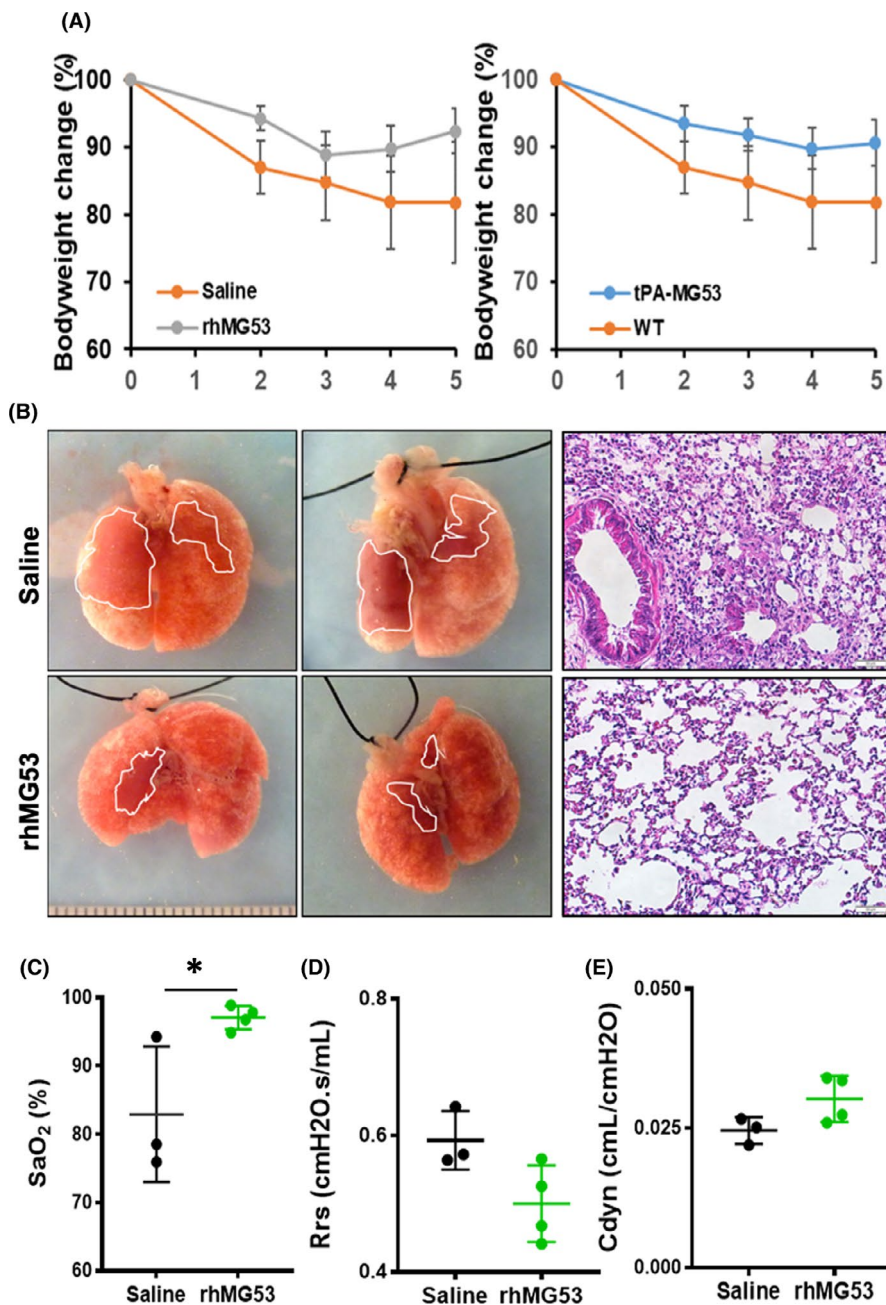


FIGURE 2 rhMG53 mitigates NM-induced lung injury. Mice were treated by intratracheal instillation of either 50 μ l NM (0.125 mg/kg in saline) or 50 μ l saline alone. After exposure, the mice were weighted daily for up to 5 days post-exposure (A). (B) Representative images (left panel) and HE staining (right panel) of saline control and rhMG53-treated (IV, 2 mg/kg) lungs subjected to NM exposure. After 5 days of exposure, the lung function was examined, and mice were euthanized for lung tissue section preparation. Quantification of the lung function with blood oxygen saturation level (SaO₂) (C), and resistance (Rrs) (D) and dynamic compliance (C_{dyn}) (E). * $p < 0.05$ for the indicated group

or pulmonary tissues).²⁸ Similar findings were also observed with PAoEC cells, where rhMG53 treatment ameliorated NM-induced ROS generation (Figure 4D). To further quantify the degree of NM-induced cell death, we conducted FACS analysis of PAoEC stained with propidium iodide (PI) and annexin V (Figure 5A). PAoEC cells that were annexin V-positive and PI-negative were defined as undergoing apoptotic cell death. As shown in Figure 5B, rhMG53 treatment improved survival of the PAoEC cells and reduced apoptotic cell death.

These findings provide a novel mechanism for NM-induced tissue injury that involves oxidative stress-mediated disruption of the cell membrane repair machinery. It also lays the foundation for the use of exogenous rhMG53 to boost the defence mechanism of these cells against vesicant-induced tissue injury.

3.5 | rhMG53 protects THP-1 cells against NM-induced injury

In addition to oxidative stress, vesicant exposure is known to cause sustained inflammation that contributes to the exacerbated and delayed lung injury. Thus, controlling inflammation is also important to combat vesicant-induced lung injury.^{2-5,7,8,14,16-18,39} We recently reported that MG53 has an anti-inflammatory role associated with tissue injury.²⁴ We found that THP-1 human macrophages express MG53 and that loss of MG53 leads to hyper-inflammation due to activation of NF- κ B.

We transfected THP-1 cells with shRNA against MG53 to generate a MG53-knockdown cell line (sh-MG53) (Figure 6). As shown in Figure 6A, sh-MG53 cells were more susceptible to NM-induced cell

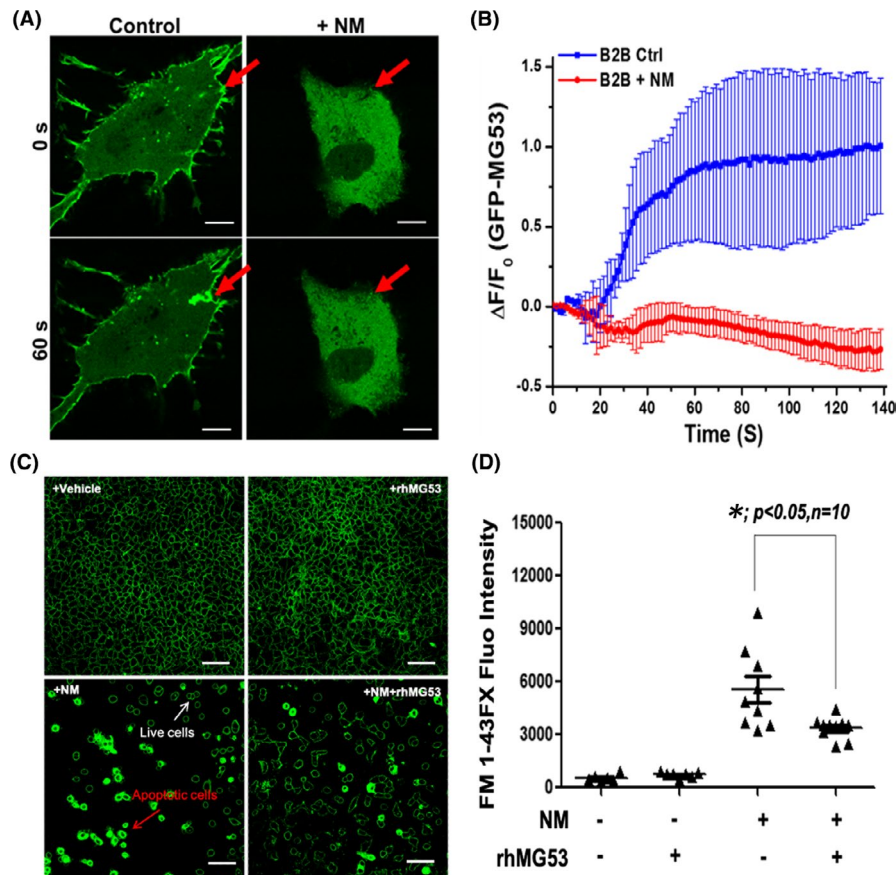


FIGURE 3 rhMG53 attenuates NM-induced membrane damage in human lung epithelial (B2B) cells. (A) The B2B cells were transfected with GFP-MG53. At 24 h after transfection, confocal fluorescence live-cell imaging was conducted with control B2B cells and those treated with 20 μ M NM, which then were injured by penetration of a microelectrode. The B2B cells show rapid translocation of GFP-MG53-containing intracellular vesicles towards the acute plasma membrane injury site following penetration of a microelectrode. Upper panel—cell image taken immediately after injury; lower panel—image taken 60 s after NM injury. Arrow shows the microelectrode injury site. Scale bar, 5 μ m. (B) Time course of GFP-MG53 accumulation at the injury sites following microelectrode penetration in NM-treated B2B cells. (C) rhMG53 treatment suppresses FM1-43FX dye entry in NM-treated B2B cells following incubation with or without rhMG53. Scale bar, 25 μ m. (D) Quantification of FM1-43 dye entry in panel c ($n = 10$)

death, compared with sh-scramble THP-1 cells. Western blot showed that NM-induced activation of caspase-3 in THP-1 cells could be reduced by the addition of exogenous rhMG53 (Figure 6B,6C). PI staining showed enhanced cell death with MG53-knockdown in THP-1 cells following NM exposure (Figure 6D). Thus, MG53 can protect against NM-induced macrophage cell death, thereby enhancing the resolution of early phase of lung injury. These findings support the anti-inflammatory function of MG53 associated with vesicant exposure.

4 | DISCUSSION

MG53 plays an essential role in cell membrane repair and pulmonary protection.^{20,21} MG53 also has anti-inflammatory function associated with chronic injury, sepsis and viral infection.^{24,25,40} In this study, we demonstrated that knockout of MG53 causes more severe lung injury and lung dysfunction following exposure to NM. Previously, we have demonstrated pulmonary pathology with the *mg53*^{-/-} mice,

which may be the underlying contributor to the increased susceptibility of the lung to NM-induced injury.²² Conversely, transgenic mice with increased levels of MG53 in the bloodstream were resistant to NM-induced tissue injuries, indicating that circulating MG53 provides critical pulmonary protection. Systemic exogenous administration of rhMG53 mitigated the adverse effects of NM-vesicant lung injury. Live-cell imaging revealed that exposure of lung epithelial cells with NM disrupts the intrinsic cell membrane repair ability of MG53, whereas the exogenous rhMG53 dampens oxidative stress caused by NM in both lung epithelial and endothelial cells. The loss of MG53 in cultured THP-1 cells lead to their increased vulnerability to vesicant-induced cell death. Together, these findings support the dual role of MG53 as a tissue-repair molecule with anti-inflammation function to protect the lungs against vesicant-induced injuries. Targeting alveolar membrane injury repair may offer an effective means to rescue the damaged lung in the acute phase of injury and to prevent the progression into the prolonged injury phase.

Through live-cell imaging, we demonstrated that, in lung epithelial cells exposed with NM, GFP-MG53 becomes immobilized

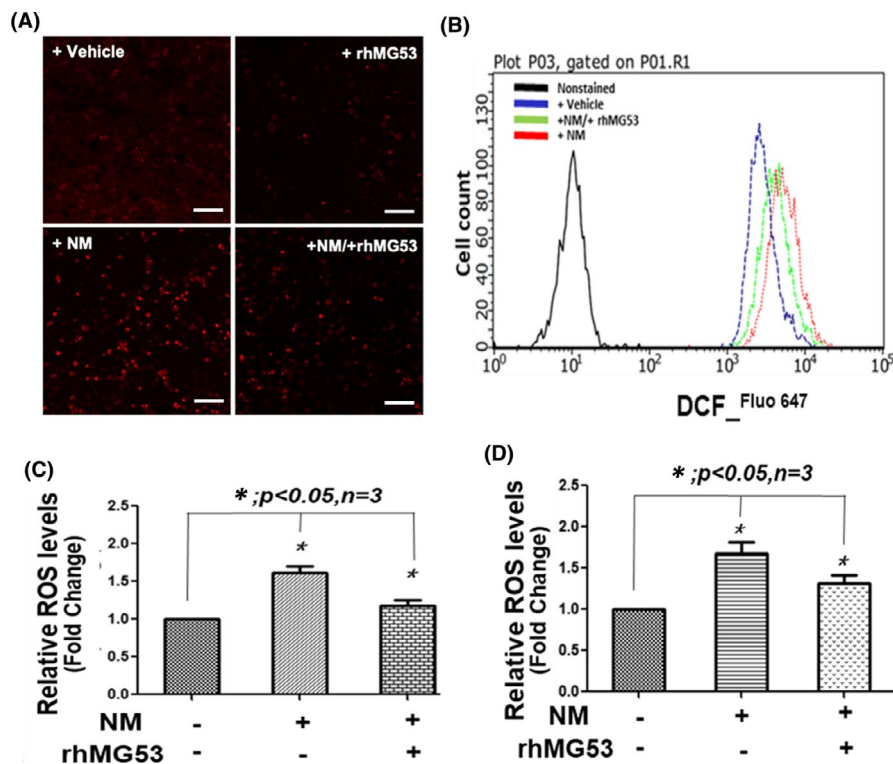


FIGURE 4 rhMG53 attenuates NM-induced oxidative stress in human bronchial epithelial (B2B) porcine aortic endothelial (PAoEC) cells. The B2B cells and primary porcine aortic endothelial (PAoEC) cells were cultured for 24 h and treated with 10 μ M (for PAoEC)/20 μ M (for B2B cells) NM or BSA control for 4 h, and washed, incubated with BSA or rhMG53 (10 μ g/ml) and cultured for another 20 h. Cells were stained and with DCF staining for ROS measurement. (A) Representative images for B2B with DCF staining. Scale bar, 25 μ m. (B) Representative FACS analysis of B2B with DCF staining; (C) Quantification of B2B (FACS) for panel b (n = 3). (D) Quantification of PAoEC for analysis with DCF staining (FACS) (n = 3)

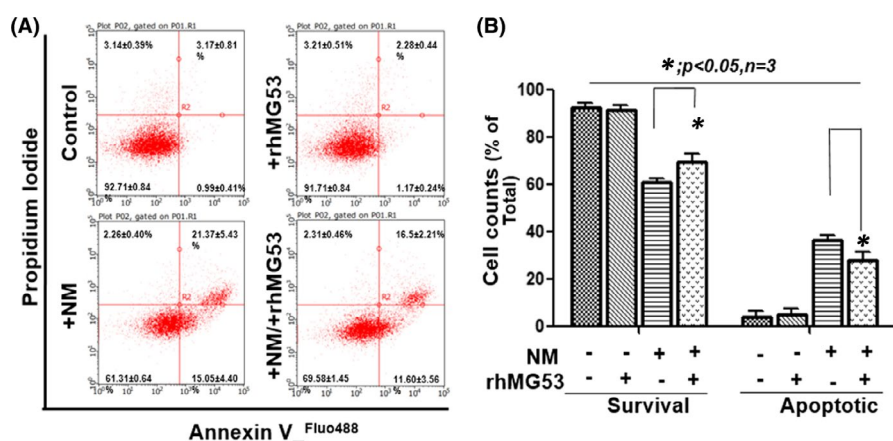


FIGURE 5 rhMG53 protects PAoEC cells from NM-induced cell death. The PAoEC cells were cultured for 24 h, treated with 10 μ M NM or BSA control for 4 h and then incubated with rhMG53 (10 μ g/ml) or BSA for another 20 h. Cells were stained analysed with annexin V and PI staining and analysed. (A) Representative apoptosis analysis of PAoEC (FACS). (B) Quantification of PAoEC apoptosis for panel a (n = 3)

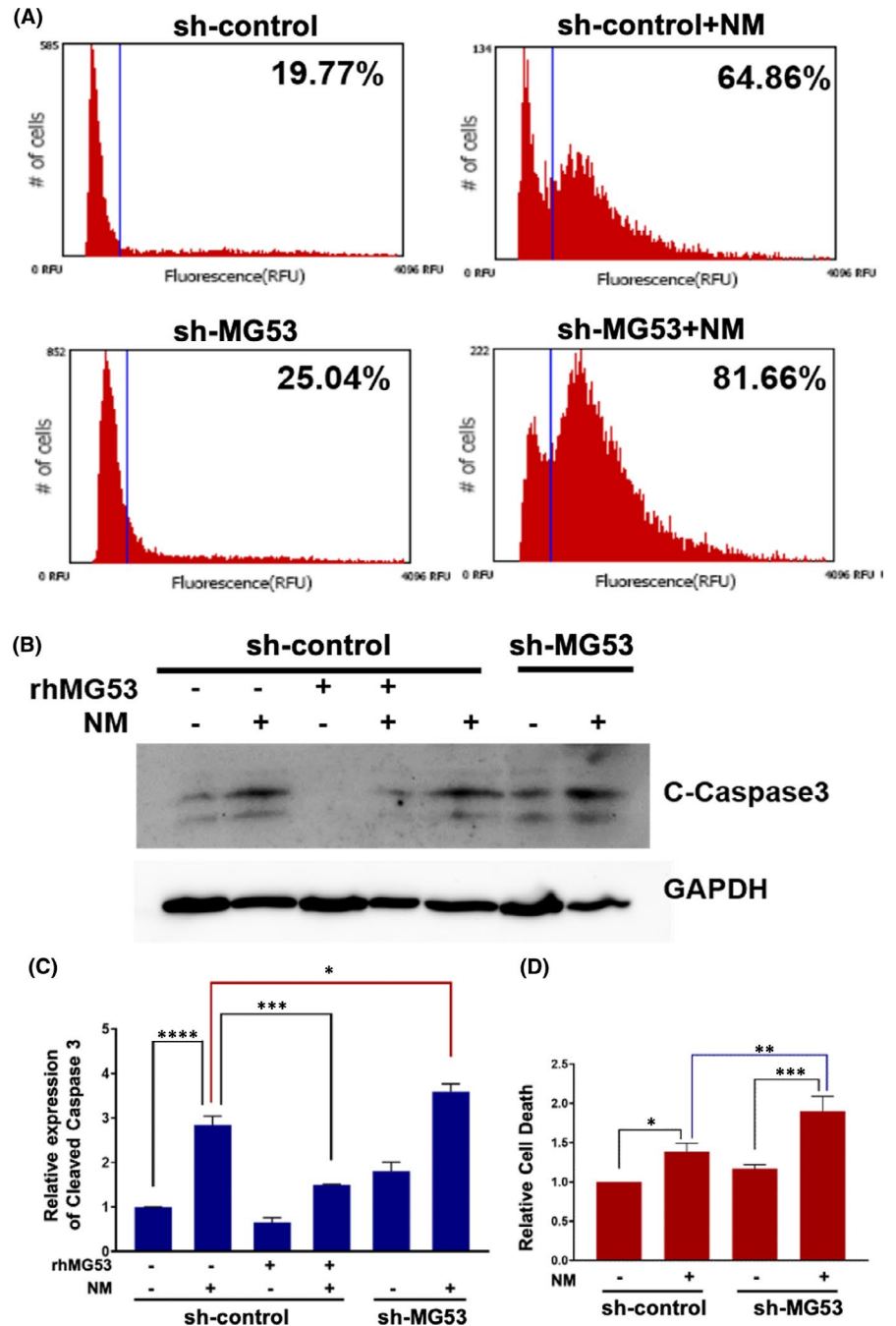
and is incapable of translocation to the membrane injury site for repair-patch formation. These findings provide direct evidence that vesicant exposure of lung epithelial cells leads to disruption of cell membrane repair machinery.

Accumulating evidence suggests that the cytotoxic mechanism associated with mustard exposure contributes to oxidative stress, which induces damage to the lung.^{6,10,11,35,36} Previously, we have demonstrated that MG53's membrane repair function is impaired when cells are subjected to chronic oxidative stress.^{37,38} The preservation of cell integrity and mitigation of oxidative stress can provide added benefits to pulmonary protection. Using cultured lung epithelial (B2B) and endothelial (PAoEC) cells, we found that rhMG53 treatment can improve survival of the cells and reduce ROS levels upon exposure to NM. These findings provide evidence that NM-induced tissue injury and oxidative stress can all be mitigated by MG53, laying the foundation for the use of exogenous

rhMG53 to boost the defence mechanism of the lungs against vesicant-induced injury.

In addition to oxidative stress, mustard gas exposure is known to induce infiltration of inflammatory cells and cytokines release in the lung that contributes to the exacerbated and delayed lung injuries.^{2,8,9,41} Macrophages are known to play a role in both acute and chronic pulmonary pathologies. An imbalance of macrophage-released pro-inflammatory and anti-inflammatory cytokines will aggravate acute lung injury and promote the development of lung toxicity.^{2,3,5,7,8,15,41} By flow cytometric analysis, we showed that THP-1 cells with knockdown of MG53 are more susceptible to NM-induced cell death, while rhMG53 treatment enhances cell survival after NM exposure. Preservation of macrophage integrity by MG53 can add to the defence mechanism of the lungs during the early phase of NM exposure. In addition to maintenance of macrophage integrity, we recently showed that repetitive administration

FIGURE 6 Knockout of MG53 results in an enhanced NM-induced cell death in THP-1 cells following NM exposure. The differentiated THP-1 cells were cultured for 24 h, treated with 10 μ M NM or BSA for 20 h and then incubated with vehicle or rhMG53 (10 μ g/ml) for another 20 h. (A) Representative image of apoptosis assay for the sh-control and sh-MG53 THP-1 cells. (B) THP-1 protein lysates were analysed by Western blot using cleaved caspase-3 and GAPDH antibody. (C) Relative expression of cleaved caspase-3. (D) Qualification of cell death with PI staining. **** $p < 0.0001$, *** $p < 0.001$, ** $p < 0.005$, $p < 0.05$ for the indicated group. Data are presented as fold changes to control basal and as mean \pm SEM ($n = 6$)



of rhMG53 could suppress the release of pro-inflammatory cytokines, for example IL-1 β and IL-6, in lung following influenza virus exposure in mice.^{24,25} The anti-inflammatory function of MG53 is associated with the control of intracellular Ca⁺⁺ oscillation and NF- κ B activation. Future studies are required to dissect the signaling cascades that are associated with vesicant-induced inflammation and the mechanisms that underlie MG53's anti-inflammatory role for the long-term benefits of lung function following vesicant exposure.

In rodents and humans, MG53 is secreted by muscle cells and is present at low levels in blood in normal physiologic conditions.^{26,42} Thus, a therapeutic approach that modulates endogenous MG53 levels/function or involves systemic administration of rhMG53

protein is potentially a safe biologic means to treat and prevent tissue damage, including vesicant-induced multi-organ injury. We have performed toxicological studies in rodents and dogs,³³ which demonstrate that rhMG53 has broad safety, underscoring its promise as a potential therapeutic to treat multi-organ injuries. Future studies testing the safety and efficacy of rhMG53 in large animal models of vesicant-induced pulmonary injury represent an essential component for our effort in translating the basic findings with MG53 into human applications.

ACKNOWLEDGEMENTS

This work was supported by NIH grants to J.M. (R01-AR070752, R01AG056919 and R01DK106394), NIH grant R01HL143000 and

Department of Defense (DOD) Army Medical Research Acquisition Activity grant W81XWH-18-1-0787 to B.A.W and NIH grant R01-HL137090 to I.D. H.L. was partially supported by the OSU Lockwood Early Career Development Award.

CONFLICT OF INTEREST

J.M. and T.T. have equity interest in TRIM-edicine, which develops MG53 for the treatment of human disease. Patents on the use of MG53 are held by Rutgers University and The Ohio State University.

AUTHOR CONTRIBUTION

Haichang Li: Conceptualization (equal); Data curation (lead); Formal analysis (lead); Investigation (lead); Methodology (equal); Project administration (equal); Supervision (equal); Validation (lead); Writing-original draft (lead); Writing-review & editing (lead). **Lucia Rosas:** Data curation (lead); Formal analysis (lead); Investigation (equal); Methodology (equal); Supervision (equal); Validation (equal). **Zhongguang Li:** Data curation (equal); Formal analysis (equal); Validation (equal). **Zehua Bian:** Data curation (supporting); Investigation (equal); Visualization (supporting). **Xiuchun Li:** Data curation (equal). **Kyoungchan Choi:** Data curation (equal). **Chuanxi Cai:** Data curation (equal). **Xinyu Zhou:** Data curation (equal); Formal analysis (equal). **Tao Tan:** Data curation (supporting). **Valerie Bergdall:** Project administration (equal); Writing-review & editing (equal). **Bryan Whitson:** Conceptualization (equal); Project administration (equal). **Ian C. Davis:** Conceptualization (equal); Data curation (lead); Methodology (equal); Project administration (equal); Supervision (equal); Writing-review & editing (equal). **Jianjie Ma:** Conceptualization (lead); Data curation (equal); Funding acquisition (lead); Investigation (lead); Project administration (lead); Supervision (lead); Writing-original draft (equal); Writing-review & editing (equal).

DATA AVAILABILITY STATEMENT

The datasets generated during the current study are available from the corresponding author upon reasonable request.

ORCID

Haichang Li  <https://orcid.org/0000-0001-9784-6480>

REFERENCES

- Smith WJ, Dunn MA. Medical defense against blistering chemical warfare agents. *Arch Dermatol*. 1991;127:1207-1213.
- Sunil VR, Patel KJ, Shen J, et al. Functional and inflammatory alterations in the lung following exposure of rats to nitrogen mustard. *Toxicol Appl Pharmacol*. 2011;250:10-18.
- Weinberger B, Laskin JD, Sunil VR, Sinko PJ, Heck DE, Laskin DL. Sulfur mustard-induced pulmonary injury: therapeutic approaches to mitigating toxicity. *Pulm Pharmacol Ther*. 2011;24:92-99.
- Weinberger B, Malaviya R, Sunil VR, et al. Mustard vesicant-induced lung injury: advances in therapy. *Toxicol Appl Pharmacol*. 2016;305:1-11.
- Malaviya R, Venosa A, Hall L, et al. Attenuation of acute nitrogen mustard-induced lung injury, inflammation and fibrogenesis by a nitric oxide synthase inhibitor. *Toxicol Appl Pharmacol*. 2012;265:279-291.
- Sunil VR, Vayas KN, Abramova EV, et al. Lung injury, oxidative stress and fibrosis in mice following exposure to nitrogen mustard. *Toxicol Appl Pharmacol*. 2020;387:114798.
- Wigenstam E, Jonasson S, Koch B, Bucht A. Corticosteroid treatment inhibits airway hyperresponsiveness and lung injury in a murine model of chemical-induced airway inflammation. *Toxicology*. 2012;301:66-71.
- Malaviya R, Sunil VR, Venosa A, et al. Inflammatory mechanisms of pulmonary injury induced by mustards. *Toxicol Lett*. 2016;244:2-7.
- Zhu XJ, Meng X, Xu R, et al. Mechanism underlying acute lung injury due to sulfur mustard exposure in rats. *Toxicol Ind Health*. 2016;32:1345-1357.
- Laskin JD, Black AT, Jan YH, et al. Oxidants and antioxidants in sulfur mustard-induced injury. *Ann N Y Acad Sci*. 2010;1203:92-100.
- Naghii MR. Sulfur mustard intoxication, oxidative stress, and antioxidants. *Mil Med*. 2002;167:573-575.
- Venosa A, Smith LC, Murray A, et al. Regulation of macrophage foam cell formation during nitrogen mustard (NM)-induced pulmonary fibrosis by lung lipids. *Toxicol Sci*. 2019;172(2):344-358. 10.1093/toxsci/kfz187
- Laskin DL, Malaviya R, Laskin JD. Role of macrophages in acute lung injury and chronic fibrosis induced by pulmonary toxicants. *Toxicol Sci*. 2019;168:287-301.
- Sunil VR, Vayas KN, Cervelli JA, et al. Pentoxifylline attenuates nitrogen mustard-induced acute lung injury, oxidative stress and inflammation. *Exp Mol Pathol*. 2014;97:89-98.
- Venosa A, Malaviya R, Gow AJ, Hall L, Laskin JD, Laskin DL. Protective role of spleen-derived macrophages in lung inflammation, injury, and fibrosis induced by nitrogen mustard. *Am J Physiol Lung Cell Mol Physiol*. 2015;309:L1487-1498.
- Malaviya R, Sunil VR, Venosa A, et al. Attenuation of nitrogen mustard-induced pulmonary injury and fibrosis by anti-tumor necrosis factor-alpha antibody. *Toxicol Sci*. 2015;148:71-88.
- Venosa A, Malaviya R, Choi H, Gow AJ, Laskin JD, Laskin DL. Characterization of distinct macrophage subpopulations during nitrogen mustard-induced lung injury and fibrosis. *Am J Respir Cell Mol Biol*. 2016;54:436-446.
- Sunil VR, Vayas KN, Cervelli JA, et al. Protective role of surfactant protein-D against lung injury and oxidative stress induced by nitrogen mustard. *Toxicol Sci*. 2018;166:108-122.
- Venosa A, Smith LC, Murray A, et al. Regulation of macrophage foam cell formation during nitrogen mustard (NM)-induced pulmonary fibrosis by lung lipids. *Toxicol Sci*. 2019;172:344-358.
- Cai C, Masumiya H, Weisleder N, et al. MG53 nucleates assembly of cell membrane repair machinery. *Nat Cell Biol*. 2009;11:56-64.
- Cai C, Weisleder N, Ko JK, et al. Membrane repair defects in muscular dystrophy are linked to altered interaction between MG53, caveolin-3, and dysferlin. *J Biol Chem*. 2009;284:15894-15902.
- Jia Y, Chen K, Lin P, et al. Treatment of acute lung injury by targeting MG53-mediated cell membrane repair. *Nat Commun*. 2014;5:4387.
- Whitson BA, Mulier K, et al. MG53 as a novel therapeutic protein to treat acute lung injury. *Mil Med*. 2021;186(Supplement_1):339-345. 10.1093/milmed/usaa313
- Sermersheim M, Kenney AD, Lin PH, et al. MG53 suppresses interferon-beta and inflammation via regulation of ryanodine receptor-mediated intracellular calcium signaling. *Nat Commun*. 2020;11:3624.
- Kenney AD, Li Z, Bian Z, et al. Recombinant MG53 protein protects mice from lethal influenza virus infection. *Am J Respir Crit Care Med*. 2021;203:254-257.
- Weisleder N, Takizawa N, Lin P, et al. Recombinant MG53 protein modulates therapeutic cell membrane repair in treatment of muscular dystrophy. *Sci Transl Med*. 2012;4:139ra185.

27. Bian ZH, Wang Q, Zhou XY, et al. Sustained elevation of MG53 in the bloodstream increases tissue regenerative capacity without compromising metabolic function. *Nat Commun*. 2019;10:4659.
28. Carrillo A, Chamorro S, Rodriguez-Gago M, et al. Isolation and characterization of immortalized porcine aortic endothelial cell lines. *Vet Immunol Immunopathol*. 2002;89:91-98.
29. Li X, He P, Wang XL, et al. Sulfiredoxin-1 enhances cardiac progenitor cell survival against oxidative stress via the upregulation of the ERK/NRF2 signal pathway. *Free Radic Biol Med*. 2018;123:8-19.
30. Aeffner F, Davis IC. Respiratory syncytial virus reverses airway hyperresponsiveness to methacholine in ovalbumin-sensitized mice. *PLoS One*. 2012;7:e46660.
31. Irvin CG, Bates JH. Measuring the lung function in the mouse: the challenge of size. *Respir Res*. 2003;4:4.
32. Li H, Duann P, Lin PH, et al. Modulation of wound healing and scar formation by MG53 protein-mediated cell membrane repair. *J Biol Chem*. 2015;290:24592-24603.
33. Duann P, Li H, Lin P, et al. MG53-mediated cell membrane repair protects against acute kidney injury. *Sci Transl Med*. 2015;7:279ra236.
34. Bian Z, Wang Q, Zhou X, et al. Sustained elevation of MG53 in the bloodstream increases tissue regenerative capacity without compromising metabolic function. *Nat Commun*. 2019;10:4659.
35. Pohanka M, Sobotka J, Jilkova M, Stetina R. Oxidative stress after sulfur mustard intoxication and its reduction by melatonin: efficacy of antioxidant therapy during serious intoxication. *Drug Chem Toxicol*. 2011;34:85-91.
36. Wahler G, Heck DE, Heindel ND, Laskin DL, Laskin JD, Joseph LB. Antioxidant/stress response in mouse epidermis following exposure to nitrogen mustard. *Exp Mol Pathol*. 2020;114:104410.
37. Li X, Jiang M, Tan T, et al. N-acetylcysteine prevents oxidized low-density lipoprotein-induced reduction of MG53 and enhances MG53 protective effect on bone marrow stem cells. *J Cell Mol Med*. 2020;24:886-898.
38. Ma H, Liu J, Bian Z, et al. Effect of metabolic syndrome on mitsugumin 53 expression and function. *PLoS One*. 2015;10:e0124128.
39. Venosa A, Gow JG, Hall L, et al. Regulation of nitrogen mustard-induced lung macrophage activation by valproic acid, a histone deacetylase inhibitor. *Toxicol Sci*. 2017;157:222-234.
40. Guan F, Huang T, Wang X, et al. The TRIM protein Mitsugumin 53 enhances survival and therapeutic efficacy of stem cells in murine traumatic brain injury. *Stem Cell Res Ther*. 2019;10:352.
41. Malaviya R, Sunil VR, Venosa A, et al. Macrophages and inflammatory mediators in pulmonary injury induced by mustard vesicants. *Ann N Y Acad Sci*. 2016;1374:168-175.
42. Zhu H, Hou J, Roe JL, et al. Amelioration of ischemia-reperfusion-induced muscle injury by the recombinant human MG53 protein. *Muscle Nerve*. 2015;52:852-858.

How to cite this article: Li H, Rosas L, Li Z, et al. MG53 attenuates nitrogen mustard-induced acute lung injury. *J Cell Mol Med*. 2022;26:1886-1895. <https://doi.org/10.1111/jcmm.16917>